

# **Large Scale Integration of Micro-Generation to Low Voltage Grids**

**Contract No: ENK5-CT-2002-00610**

**WORK PACKAGE G**

**Report**

## **Simulation Tool for Closed Loop Price Signal Based Energy Market Operation within MicroGrids**

Final Version 1.0

October 2003

*Access: Restricted to project members*

# Document Information

<b>Title</b>	Simulation Tool for Closed Loop Price Signal Based Energy Market Operation within MicroGrids
<b>Date</b>	28 <sup>th</sup> October 2003
<b>Version</b>	Draft Version 1.0
<b>Task(s)</b>	WPG TG1

<b>Coordination:</b>	Goran Strbac	<a href="mailto:goran.strbac@umist.ac.uk">goran.strbac@umist.ac.uk</a>
<b>Authors:</b>	Danny Pudjianto	<a href="mailto:danny.pudjianto@umist.ac.uk">danny.pudjianto@umist.ac.uk</a>

<b>Access:</b>	
<b>Project Consortium (for the actual version)</b> European Commission , PUBLIC (for final version)	
<b>Status:</b>	
<u><b>X</b></u>	Draft Version Final Version (internal document) Submission for Approval (deliverable) Final Version (deliverable, approved on..)

## 1. Synopsis

- 1.1. Microgrids comprise Low Voltage (LV) distribution systems with distributed electricity sources, such as micro turbines, fuel cells, photovoltaic cells, etc. together with energy storage devices, e.g. batteries, capacitors and flywheels, and controllable loads.
- 1.2. The development of microgrids has two main objectives, which are:
  - to reduce the Green House Gas (GHG) emissions by increasing the penetration of Renewable Energy Sources (RES) and other micro sources, whose the application has higher utilisation of the converted energy than the conventional power plants,
  - to increase the reliability of the electricity supply to the customers, which is apparently crucial in the nowadays electricity dependent society.
- 1.3. In order to facilitate the large penetration of small-scale distributed generations (micro sources) and energy storage devices, new operational control strategies are required since the current centrally power system control operation was not designed to handle a large number of small-scale generators.
- 1.4. It is known that the operation of short-term energy markets relates closely to the second by second technical operation of power system, therefore the market operator needs to work together with the system operator. Decentralised control strategy proposed to facilitate the operational of microgrids opens the possibility of having local short-term energy markets inside the microgrids.
- 1.5. The local micro-grid energy market can be a part of the national wholesale energy market and/or could be acting as an independent market as shown in Figure 1-1. There is also possibility that the local energy markets among microgrid cells interact with each other to form larger and more efficient electricity market.

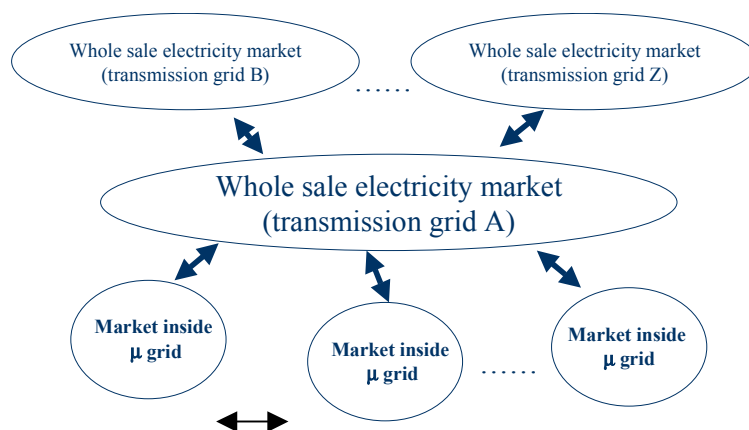


Figure 1-1 Interaction among electricity market

- 1.6. The overall aim of an energy market inside the microgrid is to promote short term cost efficient operation inside the microgrid. The operation of the microgrid in a competitive environment should open new business opportunities, which should eventually stimulate the long-term development of the microgrid components including the technology for the micro sources and other microgrid equipment.
- 1.7. However, it is still unclear whether the implementation of the local market inside the microgrids is economically and technically viable at present. The cost of developing and operating of the market must be smaller than the expected long-term benefit of having such markets in order for this concept to be economically viable. A further study needs to be conducted in order to investigate these complex issues in more detail.
- 1.8. Without implementing local energy market, the electricity production from the micro sources and the provision of ancillary services in the microgrids still somehow need to be rewarded. The dilemma is to find a suitable method of rewarding (or charging) for the provision (consumption) of those services taking into account their location and time specific contribution into the power quality and the operational security of the individual customers and the overall system.
- 1.9. Assuming that the concept of implementing local energy market inside the microgrids is economically viable, the cost of developing and running the market should be as small as possible in order to maximise the economic benefit of having such a market. In order to minimise the operational cost, it is proposed that the Micro Grid Central Controller (MGCC) will act as market and system operator simultaneously. The MGCC should be designed to run the microgrid in the automatic manner effectively removing the need for a direct human supervision.
- 1.10. As described at the WPG meeting on the 1<sup>st</sup> June 2003, a novel concept of

running the short term electricity market using closed loop price signal control strategy is proposed to be implemented in the MGCC. The controller takes into account the price information submitted by all local controllers, system limits such as voltage and thermal limits and the system requirement to balance supply and demand to determine the optimal operation of microgrids.

- 1.11. In order to verify and demonstrate the proposed concept and the developed algorithms, a simulation tool was implemented. This report describes the concept of the closed loop price signal based energy market operation, the formulation of the optimisation problem and the solution methodology implemented in the simulation tool.
- 1.12. The developed simulation tool was used to verify the technical viability of the proposed method for handling the disturbance such as changes in load in the system inside or outside the microgrids taking into account the system limits in the most economic manner. Rebalancing the demand and supply is important to mitigate the further frequency drift, which can eventually lead to a collapse of the system
- 1.13. At the end of this report, several performed case studies are discussed to investigate the operation of microgrids using the proposed control concept.

## 2. Background

- 2.1. Microgrids comprise Low Voltage (LV) distribution systems with distributed electricity sources, such as micro turbines, fuel cells, photovoltaic cells, etc. together with energy storage devices, e.g. batteries, capacitors and flywheels, and controllable loads.
- 2.2. The development of microgrids has two main objectives, which are:
  - to reduce the Green House Gas (GHG) emissions by increasing the penetration of Renewable Energy Sources (RES) and other micro sources, whose the application has higher utilisation of the converted energy than the conventional power plants,
  - to increase the reliability of the electricity supply to the customers, which is apparently crucial in the nowadays electricity dependent society.
- 2.3. In order to facilitate the large penetration of small-scale distributed generations (micro sources) and energy storage devices, new operational control strategies are required since the current centrally power system control operation was not designed to handle a large number of small-scale

generators.

- 2.4. A distributed control strategy, which comprises three critical control levels as shown in the Figure 2-1 below, should be more suitable for the microgrid application.

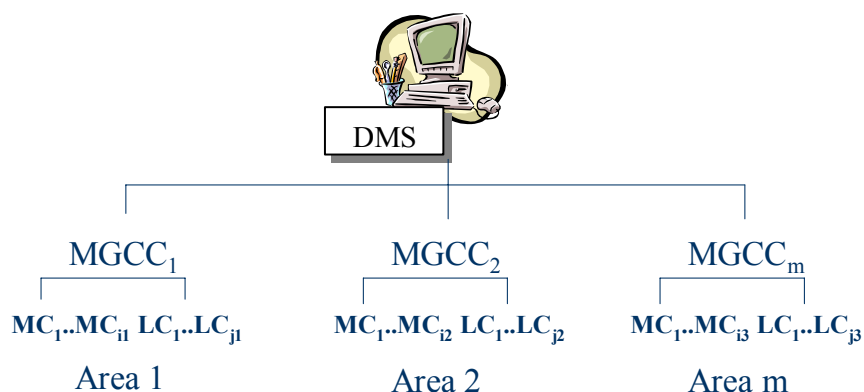


Figure 2-1 A hierarchy control architecture

- 2.5. This control structure comprises three levels:

- local Micro sources Controllers (MC) and load controllers (LC)

For each micro sources, there is a local micro source controller which has autonomy to perform local optimisation of the micro source's active and reactive production. A local micro load controller is installed at each controllable load to provide load control capabilities following instructions from the MGCC or during load shedding management.

- MicroGrid system Central Controller (MGCC)

The MGCC will be responsible to provide system load forecasts (electricity and possibly heat) and to optimise the operational of microgrids by coordinating the MCs and LCs in such a way that the economics and the security of operating the system is taken into account.

- Distribution Management System (DMS)

The DMS will work together with the MGCCs in order to operate the overall distribution system in economic and secure manner.

- 2.6. By utilising this distributed control strategy, the lower level of control can be independently operated and disconnected from the higher control hierarchy in

order to form an islanded operation as far as they have the ability to balance the supply and the demand locally with an acceptable power quality determined from the local system requirement.

- 2.7. Such control-independency enables the microgrids to be operated in one of these two operation modes; autonomous (islanding) or grid-connected mode, depending on the necessity of connecting or disconnecting the microgrids from the public distribution grids. This possibility increases the reliability of supply within the microgrids since their internal electricity resources can be used to supply their own demand during the disruption in the public grid. On the other hands, in the normal situations when the grid-connected mode is applied, the system resources including the micro sources can be utilised and shared to supply the system demand in order to achieve the maximum system economic efficiency.
- 2.8. In order to optimise operational control of microgrids and concurrently to minimise their operational cost, generating units within the microgrids need to be dispatched in the merit order fashion based on their cost of generating energy. By having the same reasons of having electricity market in the wholesale energy trading at the transmission level, the competition could be introduced at the microgrid level to promote the cost efficient operation and better business management of the microgrids, which eventually stimulates the further development of microgrids technology and applications.
- 2.9. For a successful operation, the commercial decisions taken in the electricity market must considered system limits and requirements such as power quality and security. The market itself needs to be simple, transparent and cost effective.

### 3. Closed loop price signal based energy market operation

***This approach is fully market-price driven. No load forecasting is required??!!!!***

- 3.1. Conventionally, System Operator (SO) dispatches economically the generating units in the system by instructing the generators to operate at particular levels of MW outputs. The economic despatch is calculated based on the generator cost function submitted by all generators prior to the despatch decision. The generators then are obliged to follow the SO instructions.
- 3.2. As an alternative of this operation philosophy, SO could inform the generators about the prices associated with the level of MW outputs that the SO, on the behalf of the customers, is willing to pay. The generators have the autonomy to determine the optimal level of MW outputs they are willing to produce at the given price. In order to maximise their profit, the generators will produce up to the point where their marginal cost of producing the

energy is equal to the price given by the SO.

- 3.3. Figure 2-1 shows the exchange price information between the SO, and the local controllers.

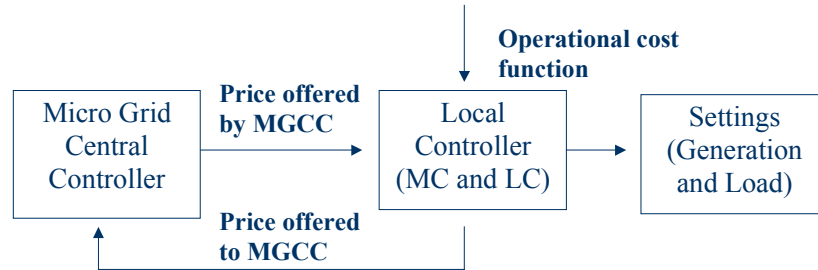


Figure 3-1 A closed loop price signal energy market

**Why do we need these steps 3.1-3.2? Who will determine Price offered by MGCC, how?**

- 3.4. MGCC, which acts as a System Operator (SO), receives the price signals (€/MWh) from each local controllers (MCs and LCs) in real time. The price signals from MCs and LCs reflects the payment asked by the generators for producing their MW output and the payment asked by the load for providing load shedding respectively. The local controllers derive the price from the predetermined given operational cost function and its operating point.

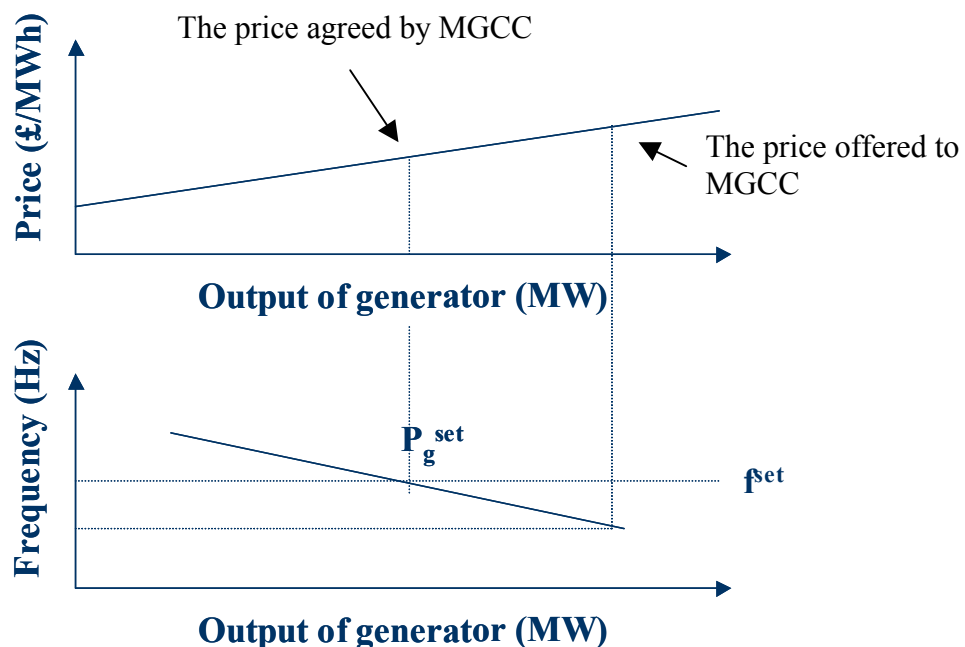


Figure 3-2 The generator price function and the generator droop characteristics

- 3.5. Figure 3-2 illustrates the generator price function and generator droop characteristics. The MCs set the  $P_g^{\text{set}}$  according to the price agreed by the

MGCC at the nominal system frequency. However, the MW output of the generator also depends on the system frequency. Once the frequency drops or rises, the generator will respond first to mitigate further drop or rise in frequency by increasing or decreasing its output automatically. The change in generator output will change the price submitted to the MGCC. MGCC needs to restore the frequency back to the nominal value in order to mitigate frequency drift, which will eventually make the system collapse.

- 3.6. The MGCC optimises the decisions based on this price information and the system requirement as constraints (voltage and thermal limits) in order to minimise the cost of operating the system. In this case, MGCC can exploit OPF algorithm to solve such optimisation problem. As results of the optimisation, a set of optimal generator dispatch is obtained concurrently with the nodal price of power injection for each node. Each local controller then receives the price offered by the MGCC based on the calculated nodal price. The MCs use this information to optimise their active power production by changing their MW output setting and the LCs determine the amount of load need to be shed based on the price offered by the MGCC. An example is given in Figure 3-3.

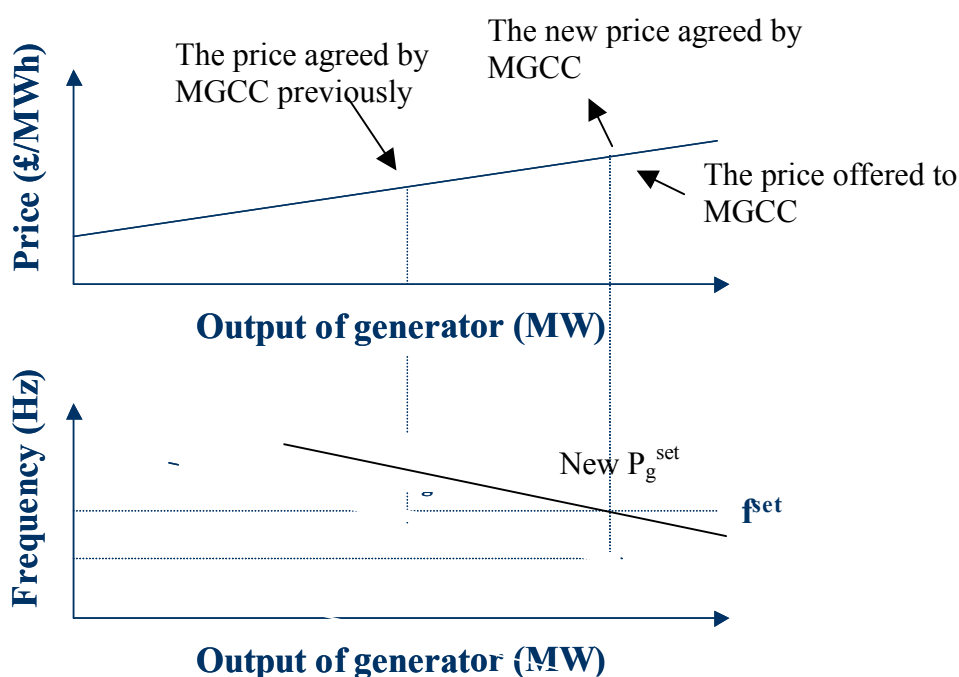


Figure 3-3 The generator price function and the generator droop characteristics

- 3.7. Assuming that the new price offered by the MC is the optimal price based on the MGCC calculation, the MGCC sends the new price signal to the MC. The MC sets the new  $P_g^{\text{set}}$  and the system frequency is restored to the nominal system frequency.

## 4. Formulation

- 4.1. In order to simulate the closed loop price signal energy market, an OPF tool was developed. The OPF problem is to minimise the cost of MW generation subject to the power balance and voltage constraints for every nodes  $i$ ; in addition, the thermal constraints for every transmission branches must not be violated.
- 4.2. In order to simplify the problem, a fixed load and a generator can form a controllable load. Both of fixed load and generator have the same capacity as the maximum load of the controllable load. Therefore, the load can be controlled to vary from zero load to the maximum load.
- 4.3. The problem can be formulated as follows.

Objective function

$$\text{Minimise } \Psi = \sum_{i=1}^{\text{MN}} (C_{p,i}^2 P_{g,i} + C_{p,i}^1 P_{g,i} + C_{p,i}^0) \quad (4.1)$$

Subject to<sup>1</sup>

1. Active power balance equation

$$P_g - P_d - \sum_{j \neq i}^{\text{MN}} FP_{ij} = 0 \quad (4.2)$$

2. Reactive power balance equation

$$Q_g - Q_d - \sum_{j \neq i}^{\text{MN}} FQ_{ij} = 0 \quad (4.3)$$

3. Voltage limit

$$V_{\min} \leq V \leq V_{\max} \quad (4.4)$$

4. Limits of active and reactive power generation

$$P_{g\min} \leq P_g \leq P_{g\max} \quad (4.5)$$

$$Q_{g\min} \leq Q_g \leq Q_{g\max} \quad (4.6)$$

---

<sup>1</sup> Since the constraints are applied to all nodes, subscript  $i$  can be dropped for the simplification purpose.

## 5. Limits of branch flows

$$S_{ij}^2 \leq S_{ij\max}^2 \quad (4.7)$$

$$S_{ji}^2 \leq S_{ji\max}^2 \quad (4.8)$$

Where

$P_g, P_d$  are the active power generation and load (MW) at node i respectively

$Q_g, Q_d$  are the reactive power generation and load (MVAR) at node i respectively

$C_p^2, C_p^l, C_p^0$  are the quadratic (€/MW<sup>2</sup>), linear (€/MW) and fixed cost (€) coefficients for active power generation at node i respectively.

$V$  is the voltage at node I (V)

$FP_{ij}, FQ_{ij}$  are the functions of the active (MW) and reactive power (MVA) flows from node I to node j respectively

$S_{ij}, S_{ji}$  are the power flows from node I to j and from j to I respectively (MVA)

MN is the number of nodes in the system

4.4. The optimisation problem is solved using an advanced Primal Dual Interior Point Method in Non Linear Programming.

## 5. Primal Dual Interior Point Method in Non Linear Programming

5.1. This section describes the solving method of the optimisation problem in section 4. The methodology is based on the Primal Dual Interior Point method in Non Linear Programming.

5.2. The method<sup>2</sup> has been proven to have superiority performance compared with other conventional optimisation methods such as Newton method, sequential quadratic programming, augmented Lagrangian, generalise reduced gradient, projected augmented Lagrangian, and etc especially in the term of the convergence speed, accuracy and the ability to handle inequality constraints.

5.3. Formulate the optimisation problem in section 4 in the form below by adding slack variables l and u as the implementation of logarithmic barrier function in order to handle the inequality constraints. l and u will provide the proximity to the variable limits, which will be used to prevent the violation of the limits during the solving process.

---

<sup>2</sup> A relatively large number of papers (more than 100's) describing this method have been published in power system analysis since 1990's.

$$\begin{aligned}
 & \text{minimise. } f(\mathbf{x}) - \mu^k \sum_{i=1}^n (\ln l_i + \ln u_i) \\
 & \text{subject to. } \mathbf{h}(\mathbf{x}) = \mathbf{0} \\
 & \quad \mathbf{g}(\mathbf{x}) - \mathbf{l} - \underline{\mathbf{g}} = \mathbf{0} \\
 & \quad \mathbf{g}(\mathbf{x}) + \mathbf{u} - \bar{\mathbf{g}} = \mathbf{0} \\
 & \quad (\mathbf{l}, \mathbf{u}) \geq \mathbf{0}
 \end{aligned} \tag{5.1}$$

Where:  $\mathbf{x} \in \mathfrak{R}^{(n)}$  is a vector of the decision variables,  
 $f(\mathbf{x})$  is an objective function,  
 $\mathbf{h}(\mathbf{x}) \equiv [h_1(\mathbf{x}), \dots, h_m(\mathbf{x})]^T$  is the vector of equality constraints,  
 $\mathbf{g}(\mathbf{x}) \equiv [g_1(\mathbf{x}), \dots, g_r(\mathbf{x})]^T$  is the vector of inequality constraints, and  
 $\bar{\mathbf{g}}$  and  $\underline{\mathbf{g}}$  are the vectors of upper and lower bounds respectively.  
 $\mu^k$  is a monotonically decrease barrier parameter along the iteration k-th. A special role of this parameter will be discussed in detail latter.

5.4. Use Langrangian function and Karush Kuhn Tucker condition (KKT) to convert the nonlinear optimisation problem into a problem of solving a set of non linear equation. The equations based on the KKT conditions can be expressed as follows.

$$\mathbf{R}_x \equiv \nabla f(\mathbf{x}) - \nabla \mathbf{h}(\mathbf{x})\mathbf{y} - \nabla \mathbf{g}(\mathbf{x})(\mathbf{z} + \mathbf{w}) = \mathbf{0} \tag{5.2}$$

$$\mathbf{R}_y \equiv \mathbf{h}(\mathbf{x}) = \mathbf{0} \tag{5.3}$$

$$\mathbf{R}_z \equiv \mathbf{g}(\mathbf{x}) - \mathbf{l} - \underline{\mathbf{g}} = \mathbf{0} \tag{5.4}$$

$$\mathbf{R}_w \equiv \mathbf{g}(\mathbf{x}) + \mathbf{u} - \bar{\mathbf{g}} = \mathbf{0} \tag{5.5}$$

$$\mathbf{KKT}_l \equiv \mathbf{L}\mathbf{Z}\mathbf{e} - \mu\mathbf{e} = \mathbf{0} \tag{5.6}$$

$$\mathbf{KKT}_u \equiv \mathbf{U}\mathbf{W}\mathbf{e} + \mu\mathbf{e} = \mathbf{0} \tag{5.7}$$

$$(\mathbf{l}, \mathbf{u}; \mathbf{z}) \geq \mathbf{0}, \mathbf{w} \leq \mathbf{0} \tag{5.8}$$

Where:  $\mathbf{R}_x, \mathbf{R}_y, \mathbf{R}_z, \mathbf{R}_w$  denote the optimality conditions associated to the gradients of the Lagrangian function in terms of primal and dual variables,

$\mathbf{KKT}_l$  and  $\mathbf{KKT}_u$  denote the complementary conditions,

$(\mathbf{L}, \mathbf{U}, \mathbf{Z}, \mathbf{W}) \in \mathfrak{R}^{(r \times r)}$  are diagonal matrices whose elements are  $\mathbf{l}, \mathbf{u}, \mathbf{z}$  and  $\mathbf{w}$  respectively,

$\mathbf{y} \in \mathfrak{R}^{(m)}$  and  $(\mathbf{z}, \mathbf{w}) \in \mathfrak{R}^{(r)}$  are the Lagrangian multipliers associated with equality and inequality constraints respectively,

$$\mathbf{e} = [1, \dots, 1]^T \in \mathfrak{R}^{(r)}.$$

5.5. Apply the perturbed Newton method to determine the descent direction for the convergence. The perturbation is required to mitigate or to reduce the possibility of being trap in the one of variable limits prematurely.

$$(\nabla^2 \mathbf{h}(\mathbf{x})\mathbf{y} + \nabla^2 \mathbf{g}(\mathbf{x})(\mathbf{z} + \mathbf{w}) - \nabla^2 f(\mathbf{x}))\Delta \mathbf{x} + \nabla \mathbf{h}(\mathbf{x})\Delta \mathbf{y} + \nabla \mathbf{g}(\mathbf{x})(\Delta \mathbf{z} + \Delta \mathbf{w}) = \mathbf{R}_{x_0} \quad (5.9)$$

$$\nabla \mathbf{h}(\mathbf{x})^T \Delta \mathbf{x} = -\mathbf{R}_{y_0} \quad (5.10)$$

$$\nabla \mathbf{g}(\mathbf{x})^T \Delta \mathbf{x} - \Delta \mathbf{l} = -\mathbf{R}_{z_0} \quad (5.11)$$

$$\nabla \mathbf{g}(\mathbf{x})^T \Delta \mathbf{x} + \Delta \mathbf{u} = -\mathbf{R}_{w_0} \quad (5.12)$$

$$\mathbf{Z}\Delta \mathbf{l} + \mathbf{L}\Delta \mathbf{z} = -\mathbf{R}_{l_0}^\mu \quad (5.13)$$

$$\mathbf{W}\Delta \mathbf{u} + \mathbf{U}\Delta \mathbf{w} = -\mathbf{R}_{u_0}^\mu \quad (5.14)$$

Where:  $\mathbf{R}_{x_0}$ ,  $\mathbf{R}_{y_0}$ ,  $\mathbf{R}_{l_0}^\mu$ ,  $\mathbf{R}_{u_0}^\mu$ ,  $\mathbf{R}_{z_0}$ , and  $\mathbf{R}_{w_0}$  represent the residuals of the perturbed KKT equations.

$\nabla^2 \mathbf{h}(\mathbf{x})$  and  $\nabla^2 \mathbf{g}(\mathbf{x})$  are Hessian matrices of  $\mathbf{h}(\mathbf{x})$  and  $\mathbf{g}(\mathbf{x})$ .

5.6. By substituting  $\Delta \mathbf{l}$ ,  $\Delta \mathbf{u}$ ,  $\Delta \mathbf{z}$  and  $\Delta \mathbf{w}$  in Equation (5.9) with Equations (5.15)-(5.16), reduced set of system equations in Equations (5.17)-(5.18) can be obtained.

$$\begin{cases} \Delta \mathbf{l} = \nabla \mathbf{g}(\mathbf{x})^T \Delta \mathbf{x} + \mathbf{R}_{z_0} \\ \Delta \mathbf{u} = -(\nabla \mathbf{g}(\mathbf{x})^T \Delta \mathbf{x} + \mathbf{R}_{w_0}) \end{cases} \quad (5.15)$$

$$\begin{cases} \Delta \mathbf{z} = -\mathbf{L}^{-1} \mathbf{Z} \nabla \mathbf{g}(\mathbf{x})^T \Delta \mathbf{x} - \mathbf{L}^{-1} (\mathbf{Z} \mathbf{R}_{z_0} + \mathbf{R}_{l_0}^\mu) \\ \Delta \mathbf{w} = \mathbf{U}^{-1} \mathbf{W} \nabla \mathbf{g}(\mathbf{x})^T \Delta \mathbf{x} + \mathbf{U}^{-1} (\mathbf{W} \mathbf{R}_{w_0} - \mathbf{R}_{u_0}^\mu) \end{cases} \quad (5.16)$$

$$\begin{bmatrix} \mathbf{H}(\bullet) & \mathbf{J}(\mathbf{x})^T \\ \mathbf{J}(\mathbf{x}) & \mathbf{0} \end{bmatrix} \begin{bmatrix} \Delta \mathbf{x} \\ \Delta \mathbf{y} \end{bmatrix} = - \begin{bmatrix} \Psi(\bullet, \mu) \\ \mathbf{h}(\mathbf{x}) \end{bmatrix}$$

Note: (5.17)

Form of linear equation:  $\mathbf{A} \cdot \mathbf{x} = \mathbf{b}$ ,  $\mathbf{A}$  is the constraint matrix,  $\mathbf{x}$  is the solution vector and  $\mathbf{b}$  is a vector of right hand side (rhs)

where:

$$\begin{cases} \mathbf{H}(\bullet) \equiv \mathbf{H}_h + \mathbf{H}_g = (\nabla^2 \mathbf{h}(\mathbf{x})\mathbf{y} + \nabla^2 \mathbf{g}(\mathbf{x})(\mathbf{z} + \mathbf{w}) - \nabla^2 f(\mathbf{x})) + \nabla \mathbf{g}(\mathbf{x}) \mathbf{S} \nabla \mathbf{g}(\mathbf{x})^T \\ \mathbf{S} = \mathbf{U}^{-1} \mathbf{W} - \mathbf{L}^{-1} \mathbf{Z} \\ \mathbf{J}(\mathbf{x}) \equiv \nabla \mathbf{h}(\mathbf{x}) \\ \Psi(\bullet, \mu) \equiv -\mathbf{R}_{x_0} - \nabla \mathbf{g}(\mathbf{x}) (\mathbf{U}^{-1} (\mathbf{W} \mathbf{R}_{w_0} - \mathbf{R}_{u_0}^\mu) - \mathbf{L}^{-1} (\mathbf{Z} \mathbf{R}_{z_0} + \mathbf{R}_{l_0}^\mu)) \\ = \nabla \mathbf{h}(\mathbf{x})\mathbf{y} - \nabla f(\mathbf{x}) + \nabla \mathbf{g}(\mathbf{x}) (\mathbf{U}^{-1} \mathbf{W} \mathbf{R}_{w_0} - \mathbf{L}^{-1} \mathbf{Z} \mathbf{R}_{z_0} - \mu (\mathbf{U}^{-1} - \mathbf{L}^{-1})) \end{cases} \quad (5.18)$$

5.7. The PDIPM algorithm [????], which will be used to solve the problem, can be summarised as follows:

*Step 0:* Initialisation: Set  $k=1$ ,  $K_{\max}=200$ , centring parameter  $\sigma \in (0,1]$ , and convergence criteria, calculate  $r$  = number of inequality constraints, choose  $\mathbf{u}, \mathbf{l} > \mathbf{0}$  and  $\mathbf{z} > \mathbf{0}, \mathbf{w} < \mathbf{0}, \mathbf{y} = \mathbf{0}$ , where  $k$ ,  $K_{\max}$  are the iteration counter and its maximum respectively.

WHILE ( $k < K_{\max}$ ) DO:

*Step 1:* Compute the complementary gap:

$$C_{\text{gap}} \equiv \sum_{i=1}^r l_i z_i - u_i w_i \quad (5.19)$$

If the convergence criteria, which comprises the maximum of active and reactive mismatched and complementary gap, is satisfied, then the current result is considered as the optimal solution and the iterative process can be stopped.

*Step 2:* Compute the perturbed factor

$$\mu \equiv \sigma \frac{C_{\text{gap}}}{2r} \quad (5.20)$$

*Step 3:* Solve Equation (5.17) for  $[\Delta \mathbf{x}, \Delta \mathbf{y}]$

*Step 4:* Given  $\Delta \mathbf{x}$ , calculate  $\Delta \mathbf{l}, \Delta \mathbf{u}$  and  $\Delta \mathbf{z}, \Delta \mathbf{w}$  using Equations (5.15) and (5.16) respectively.

*Step 5:* Perform the ratio test to determine the maximum step length in the primal and dual space:

$$\text{step}_p = 0.9995 \min \left\{ \min_i \left( \frac{-l_i}{\Delta l_i} \text{ when } \Delta l_i < 0; \frac{-u_i}{\Delta u_i} \text{ when } \Delta u_i < 0 \right), 1 \right\} \quad (5.21)$$

$$\text{step}_D = 0.9995 \min \left\{ \min_i \left( \frac{-z_i}{\Delta z_i} \text{ when } \Delta z_i < 0; \frac{-w_i}{\Delta w_i} \text{ when } \Delta w_i > 0 \right), 1 \right\} \quad (5.22)$$

Note that direct update of the variables using the increment found in steps 3 and 4, cannot be used as it may result in a violation of the constraints. Consider a variable  $d$  such that  $d \geq 0$ . Suppose that the increment at the  $k$ -th iteration is negative,  $\Delta d^k \leq 0$ . In order to enforce non-negativity of the variable,  $d^{(k+1)} = d^{(k)} + \text{step} \Delta d^k \geq 0$ , the parameter  $\text{step}$  must satisfy the

following condition,  $step \leq \frac{-d^{(k)}}{\Delta d^{(k)}}$ . In order to ensure the numerical stability of the algorithm,  $step$  is calculated as  $step = 0.9995 \frac{-d^{(k)}}{\Delta d^{(k)}}$

Step 6: Update the primal and dual variables by:

$$\begin{bmatrix} \mathbf{x} \\ \mathbf{l} \\ \mathbf{u} \end{bmatrix}^{k+1} = \begin{bmatrix} \mathbf{x} \\ \mathbf{l} \\ \mathbf{u} \end{bmatrix}^k + step_p \begin{bmatrix} \Delta \mathbf{x} \\ \Delta \mathbf{l} \\ \Delta \mathbf{u} \end{bmatrix}^k ; \begin{bmatrix} \mathbf{y} \\ \mathbf{z} \\ \mathbf{w} \end{bmatrix}^{k+1} = \begin{bmatrix} \mathbf{y} \\ \mathbf{z} \\ \mathbf{w} \end{bmatrix}^k + step_D \begin{bmatrix} \Delta \mathbf{y} \\ \Delta \mathbf{z} \\ \Delta \mathbf{w} \end{bmatrix}^k \quad (5.23)$$

Step 7: Increase index k by 1

END DO

Step 8: Print “Computation does not converge”.

Step 8 indicates the non-convergence of the iterative process. The problem needs to be investigated further to find the causes of the convergence problem.

## 6. Case study

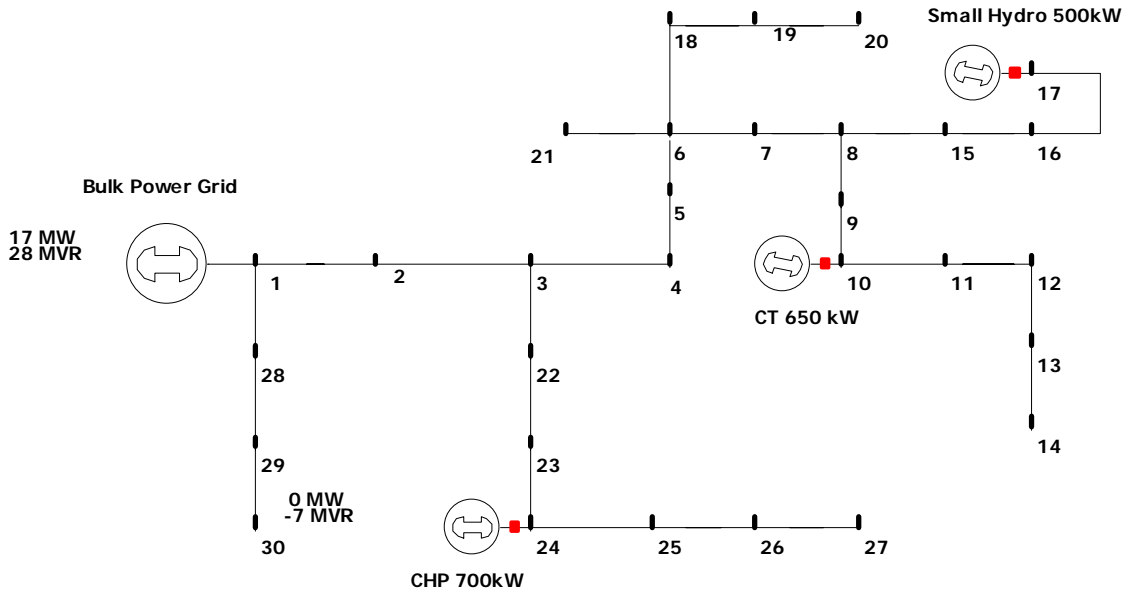


Figure 6-1 30 bus radial test system

6.1. A 30-bus radial test system shown in Figure 6-1 was used to simulate the application of the closed loop price signal based short-term energy market operation. The test system corresponds to a MV network and is used only for the purpose of demonstrating the concept of the proposed control strategy and the developed tool. In the future, LV test systems need to be developed.

However, for the purpose of this study, the test system is still appropriate.

- 6.2. For the sake of simplicity, a lossless and unconstrained network was assumed in this study. However, losses and network constraints have been considered in the formulation in section 4.
- 6.3. This system has a total load of 14.20 MW and 5 MVar and it has three distributed generators with different size of capacity and droop characteristics connected to the network at particular nodes.
- 6.4. A generator connected to bus 1, which also acted as a slack bus, was a representation of the supply from the public distribution grid.
- 6.5. All network data and the generators' parameters can be found in the Appendix A. It is important to note that the generators' parameters may not reflect the realistic generator parameter; the parameters were arbitrarily determined for the sake of study.
- 6.6. The simulation scenario was as follows. First, the system states and the optimal generation despatch were calculated and the nodal prices in the system were observed. Second, the MW load at bus 21 was increased from 200 kW to 400 kW at  $t=2$  min. The responds from each generator and the MGCC due to the increase in system loading, the restoration of the dropped frequency and the convergence of the system marginal price to the new steady state value were observed.
- 6.7. In this scenario, the MGCC evaluated the system condition in every minute. Since the size of microgrids are relatively small, the computation time required for the MGCC to solve the OPF problem is likely to be fast enough, less than few seconds with the current available reasonable modern computer (min. 500 MHz CPU).

**Table 6-1 The initial steady states condition**

Bus	Voltage (p.u.)	Angle (degree)	PL (MW)	QL (MVar)	PG (MW)	QG (MVar)	Nodal Price (€/MWh)
1	1.050	0.00	0.0	0.0	13.0	5.3	34.02
2	1.050	-0.01	0.5	0.2	0.0	0.0	34.02
3	1.047	-0.37	0.0	0.0	0.0	0.0	34.02
4	1.043	-1.00	0.9	0.3	0.0	0.0	34.01
5	1.042	-1.25	0.0	0.0	0.0	0.0	34.01
6	1.039	-1.73	0.0	0.0	0.0	0.0	34.00
7	1.037	-2.00	0.0	0.0	0.0	0.0	34.00
8	1.035	-2.26	0.0	0.0	0.0	0.0	34.00
9	1.033	-2.43	0.2	0.1	0.0	0.0	33.99
10	1.032	-2.59	0.0	0.0	0.4	-0.3	33.99
11	1.028	-3.16	0.3	0.1	0.0	0.0	33.98
12	1.027	-3.40	0.7	0.2	0.0	0.0	33.97
13	1.026	-3.46	0.8	0.3	0.0	0.0	33.97

Bus	Voltage (p.u.)	Angle (degree)	PL (MW)	QL (MVA <sub>r</sub> )	PG (MW)	QG (MVA <sub>r</sub> )	Nodal Price (€/MWh)
14	1.026	-3.53	0.7	0.2	0.0	0.0	33.97
15	1.034	-2.30	0.5	0.2	0.0	0.0	33.99
16	1.034	-2.33	0.5	0.2	0.0	0.0	33.99
17	1.033	-2.34	0.5	0.2	0.4	-0.3	33.99
18	1.038	-1.80	0.4	0.1	0.0	0.0	34.00
19	1.037	-1.96	0.7	0.2	0.0	0.0	34.00
20	1.037	-2.01	0.5	0.2	0.0	0.0	34.00
21	1.039	-1.75	0.2	0.1	0.0	0.0	34.00
22	1.045	-0.62	0.5	0.2	0.0	0.0	34.02
23	1.044	-0.76	1.9	0.6	0.0	0.0	34.02
24	1.043	-0.86	0.0	0.0	0.4	-0.3	34.01
25	1.041	-1.17	1.1	0.4	0.0	0.0	34.01
26	1.041	-1.29	0.5	0.2	0.0	0.0	34.01
27	1.040	-1.36	0.8	0.3	0.0	0.0	34.01
28	1.050	-0.01	0.1	0.3	0.0	0.0	34.02
29	1.049	-0.17	0.9	0.3	0.0	0.0	34.02
30	1.049	-0.22	0.9	0.3	0.0	0.0	34.01

6.8. Table 6-1 shows the voltage magnitude and angle, the active and reactive power load and generation, and the active power nodal price for each node. As expected in the lossless and unconstrained network that the optimality is found when the nodal prices are equal. In this case, the nodal prices converged to around 34 €/MWh.

6.9. At  $t = 2$  min, the load at bus 21 was increased from 200 kW to 400 kW.

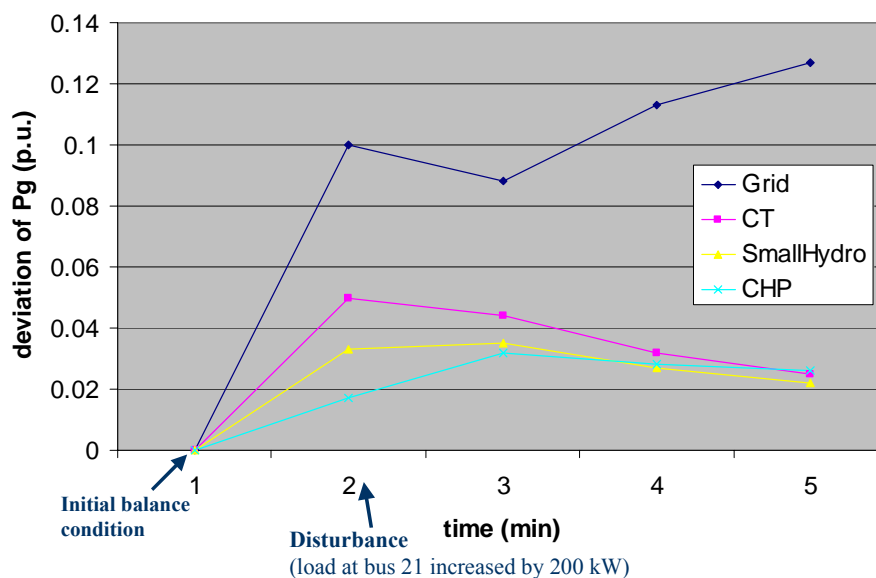


Figure 6-2 Deviation of generators' active power output

6.10. Figure 6-2 illustrates the deviation of generators' active power output responding the increase in system loading. Following the increase, generators were responding automatically according their droop characteristics. The increment of supply from the distribution grid is the largest since the

generator represented the grid has the lowest droop characteristics and hence provides the fastest frequency response. In contrast, CHP at bus 24 provides the slowest frequency response and hence the increment of MW production from CHP is the lowest one.

- 6.11. In practice, the increment of the generation will be between  $t=2$  and  $t=3$  assuming that the generation can achieved the new steady state operating point in less than 1 minute. In this simulation, the operating point was calculated in discrete manner (every 1 minute) and therefore it was assumed that the generators can react and achieve the steady state operating point directly. However, for the purpose of investigating the system behaviour when the proposed method is applied, this assumption is likely to be acceptable. If necessary, further analysis using complex OPF in dynamic analysis may need to be done.

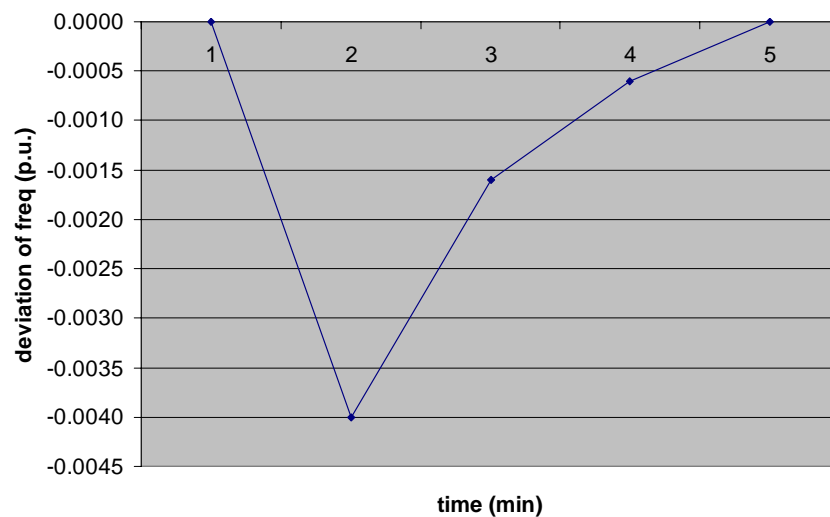


Figure 6-3 Frequency deviation

- 6.12. Figure 6-3 shows the restoration of the system frequency, which fell down right after the increase in the loading at bus 21. At  $t=2$ , the frequency dropped up to 0.004 p.u. and it was restored gradually when generators started to respond by increasing the setting of their MW production. At  $t=5$ , the frequency achieved the same value as before the disturbance.

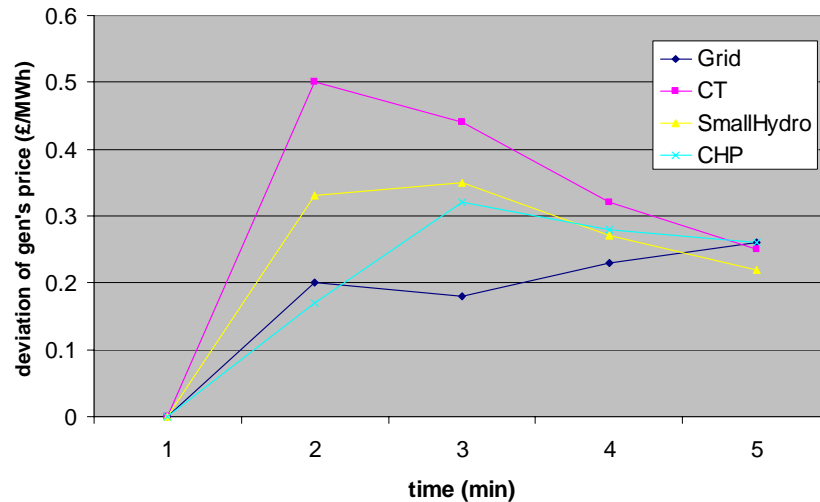


Figure 6-4 Increase of nodal prices at generation nodes

6.13. Figure 6-4 shows the deviation of the nodal prices submitted by the local controllers (MCs) to the MGCC from the previous steady state condition. At  $t=2$ , the prices were totally determined by the generator droop characteristics. At  $t=5$ , the prices converged to the new system marginal price around €34.25/MWh.

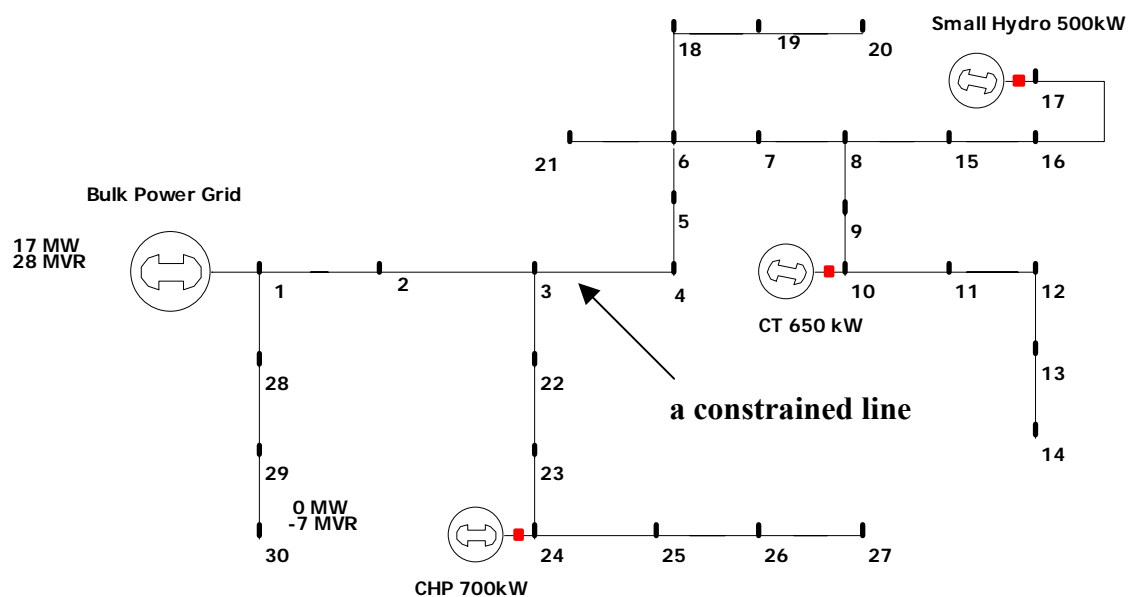


Figure 6-5 30 bus radial test system

6.14. The second case study investigated the performance of the proposed control method to handle the increase load at bus 21 from 200 kW to 400 kW at  $t=2$  min taking into account the system limits such as thermal limit. Line 3 – 4 has maximum physical ability to transfer 6.5 MVA power flows. The same

observations were done as the previous study.

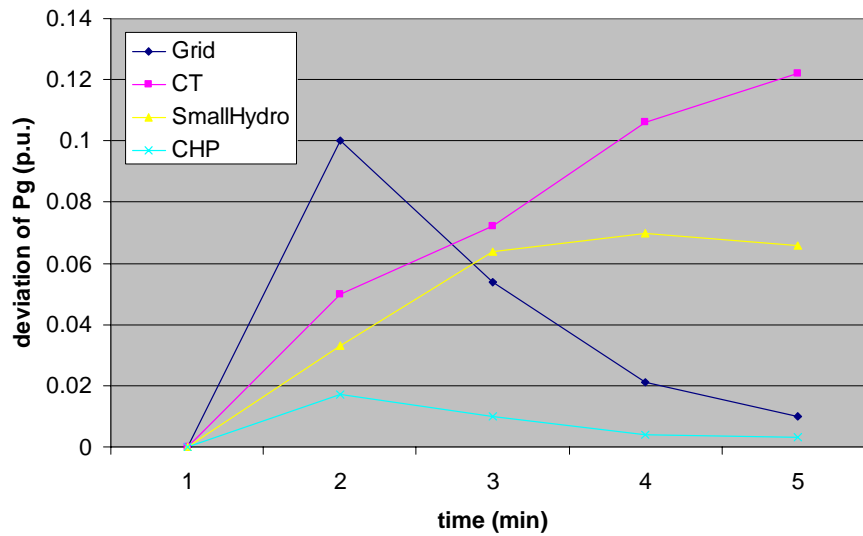


Figure 6-6 Deviation of generators' active power output

- 6.15. Following the increase in loading at bus 21, generators initially have the same respond driven by their droop characteristics as the previous case study. However, considering the thermal constraint at line 3-4, MW production of each generator converged to different values as in the previous case study.

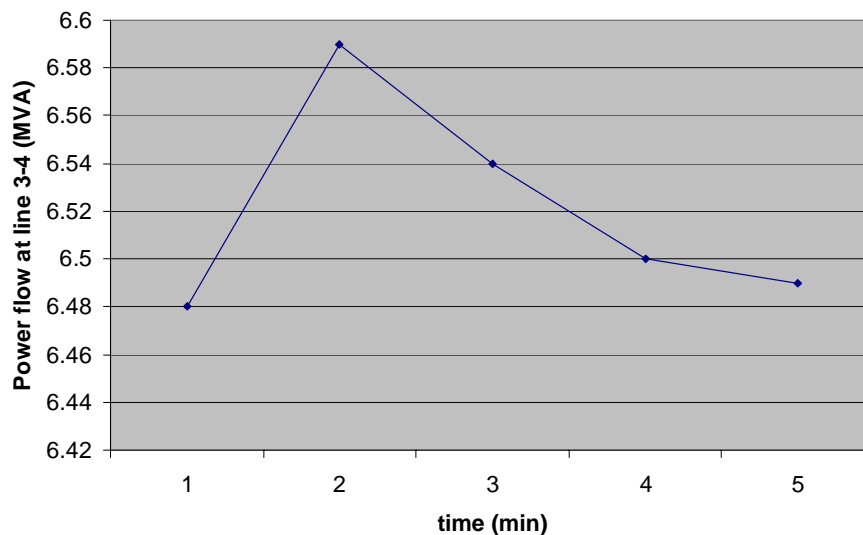


Figure 6-7 Power flow at line 3-4

- 6.16. Figure 6-7 shows the power flows at line 3-4. At  $t=2$ , the thermal limit of line 3-4 was violated. Following the respond of each generators to the price signals from MGCC, the despatch was changed in such a way that the violation of thermal constraint was gradually reduced until there was no violation at  $t=5$  min.

6.17. The previous despatch did not take into account system security and therefore the corrective action required the violation of the thermal constraint for a period of time. If needed, then the security can be implemented in the formulation taking into account the possibility of increase in system loading or changing in the generation or the network outages.

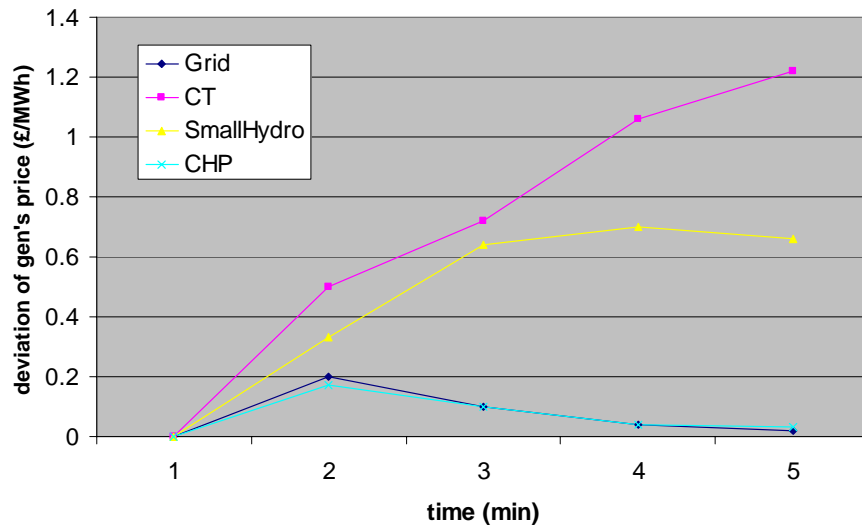


Figure 6-8 Increase of nodal prices at generation nodes

6.18. Figure 6-8 shows the deviation of the prices submitted by the MCs to the MGCC. In contrast to the result in the previous case study when the nodal prices converged into one system marginal price, in this case the nodal prices unsurprisingly converged to different values, as the thermal constraint for line 3-4 becomes an active constraint.

6.19. The MW production from generators which contribute to the reduction of thermal violation, i.e. CT and small hydro would be selected instead of the MW from the generators which contribute to the increase of thermal violation, i.e. supply from the grid and CHP despite the fact that CT and small hydro, in this case, asked higher prices than CHP and supply from grid.

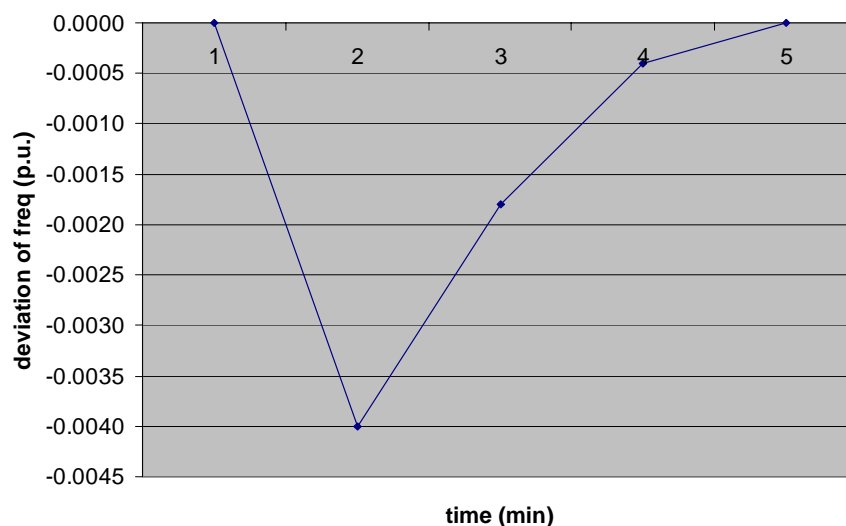


Figure 6-9 Frequency deviation

6.20. Figure 6-9 shows the restoration of the dropped frequency after the increase load at bus 21. At  $t=5$ , the frequency was restored to the same frequency prior to the disturbance.

## 7. Summary and Future Works

7.1. The concept of closed loop price signal based short- term energy market operation seems to be reasonably working for energy balancing the system taking into account the economy efficiency and the system limits.

7.2. However, further studies are still needed in the following areas:

- the performance of the method to integrate the operation of local controllers (LCs and) MCs, and the operation of storage devices.
- To deal with the intermittent and non fully controllable generators such as wind farms, and PV.
- To coordinate economically the supply of the heat and electrical demand.

## 8. References

1. MicroGrids Workgroup, “Large Scale Integration of Micro Generation to Low Voltage Grids – Target Action 1: Annex 1 “Description of Work”, Athens, May, 2002.

2. Cardell, J. and Ilic, M., “ The control and operation of distributed generation in a competitive electricity market”, Power System Restructuring: Engineering and Economics, Kluwer Academic Publishers, 1998.
3. Wei, H., Sasaki, H., Kubokawa, J., and Yokoyama, R., "An interior point nonlinear programming for optimal power flow problems with a novel data structure," IEEE Transactions on Power Systems, vol. 13, no. 3, pp. 870-877, 1998.
4. Quintana, V. H., Torres, G.L., Palomo, J.M.,” Interior Point Methods and their applications to power systems: a classification of publications and software codes,” IEEE Trans. on Power Systems, vol. 15, no. 1, pp. 170-176, 2000.
5. Momoh, J. A., El Hawary, M. E., and Adapa, R., "A review of selected optimal power flow literature to 1993 part I: NonLinear and quadratic programming approaches," IEEE Transactions on Power Systems, vol. 14, no. 1, pp. 96-104, 1999.
6. Momoh, J. A., El Hawary, M. E., and Adapa, R., "A review of selected optimal power flow literature to 1993 part II: Newton, linear programming and interior point methods," IEEE Transactions on Power Systems, vol. 14, no. 1, pp. 105-111, 1999.

## Appendix A

### Data of 30 Bus radial test system

Voltage base: 23 kV  
MVA base: 100 MVA

#### Bus data

Bus	P load (kW)	Q load (kVAr)	Bus	P load (kW)	Q load (kVAr)
1	0	0	16	549	183
2	522	174	17	477	159
3	0	0	18	432	144
4	936	312	19	672	224
5	0	0	20	495	165
6	0	0	21	207	69
7	0	0	22	522	174
8	0	0	23	1917	639
9	189	63	24	0	0
10	0	0	25	1116	372
11	336	112	26	549	183
12	657	219	27	792	264
13	783	261	28	82	294
14	729	243	29	882	294
15	477	159	30	882	294

Note: Bus 1 is a slack bus

#### Network data

Bus I	Bus j	R(pu)	X(pu)	Bus I	Bus j	R(pu)	X(pu)
1	2	0.041418	0.0022306	16	17	0.246749	0.1389981
2	3	0.065879	0.0651418	6	18	0.091456	0.0795085
3	4	0.222117	0.1930813	18	19	0.300529	0.2612098
4	5	0.104537	0.0908507	19	20	0.290907	0.1638752
5	6	0.314272	0.1770321	6	21	0.114329	0.0993762
6	7	0.255312	0.1438185	3	22	0.106597	0.1053875
7	8	0.255312	0.1438185	22	23	0.064877	0.0641399
8	9	0.250643	0.1411909	23	24	0.10828	0.0941210
9	10	0.250643	0.1411909	24	25	0.27603	0.2399244
10	11	0.750643	0.4228544	25	26	0.200888	0.1746125
11	12	0.350643	0.1975236	26	27	0.285709	0.1609452
12	13	0.142854	0.0804726	1	28	0.088072	0.0096408
13	14	0.290907	0.1638752	28	29	0.309093	0.1741210
8	15	0.08983	0.0780907	29	30	0.210643	0.1186578
15	16	0.137656	0.0775425				

#### Generator data

Bus	Pmin (kW)	Pmax (kW)	Qmin (kVAr)	Qmax (kVAr)	$C_p^2$ (€/MW <sup>2</sup> )	$C_p^1$ (€/MW)	$C_p^0$ (€)	Droop
1	-9999	9999	-9999	9999	1	8	0	0.04
10	0	650	-300	300	5	30	0	0.08
17	0	500	-300	300	5	30	0	0.12
24	0	700	-300	300	5	30	0	0.24